ISBN: 978-3-95450-214-1 ISSN: 2673-5490 doi:10.18429/JACoW-IPAC2021-WEPAB102

HALF-METAL SPIN FILTER FOR HIGHLY POLARIZED EMISSION FROM GaAs PHOTOCATHODES

S. Poddar†, C. Jing, E. J. Montgomery, Euclid Beamlabs, LLC, Bolingbrook, USA
M. Stutzman, S. Zhang, Thomas Jefferson National Lab., Newport News, USA
C. Palmstrøm, University of California, Santa Barbara, USA
P. Lukashev, University of Northern Iowa, Cedar Falls, USA

Abstract

Strained gallium arsenide photocathodes are one of the major sources of spin-polarized electrons. Ultrathin epitaxial half-metal (HM) Heusler alloys as spin filters were grown on GaAs photocathodes. Epitaxial layers of Heusler alloy half-metals have 100% spin ordering that can be easily switched using a low magnetic field. Besides, they are closely lattice matched with GaAs. Electrons with spin along the same direction as the spin-filter pass while all the others are scattered in the bulk producing a beam of near-100% polarized electrons. In Phase I, extensive first-principle electronic calculations using standard Density Functional Theory (DFT) were performed to predict possible Heusler alloy half-metal candidates to be used as a spin-filter. Several devices were experimentally fabricated using dedicated molecular beam epitaxy growth system. As a proof of principle, we implemented quantum efficiency and polarization testing of these half-metal/GaAs heterostructures using a dedicated Mott polarimeter. Photoemission was observed for both magnetically switched antiparallel spin-filter directions which is a qualitative proof of the concept proposed in Phase I and may lead to further device optimization and upgraded polarimeter design.

DFT MODELING OF HALF-METALS

The main goal of the DFT simulation was identification and theoretical study of potential half-metallic (HM) Heusler compounds that could be used in multilayer geometry with gallium arsenide for production of highly spin-polarized electrons. HM are characterized by a metallic band structure for one spin direction and an insulating band structure for the opposite. HM materials exhibit an integer value of the spin moment (due to the integer number of bands separated by the energy gap) and metallic conductivity. Half-metallicity has been reported in spinels, Heusler (and half-Heusler) compounds, double-perovskites, as well as in the binary compound CrO_2. Despite some challenges, such as low magnetic ordering temperature, and potentially detrimental effects of interface / surface states, half-metals are considered one of the primary candidates for device applications in spintronics [1].

Half-metallic Heusler alloys are among the most promising candidates for applications in spintronics, as they could exhibit a complete spin polarization at room temperature. These materials have been intensively studied in recent years, with many systems being suggested to exhibit a 100% spin-polarization. The spin polarization is defined as:

$$P = \big(N_\uparrow(E_F) - N_\downarrow(E_F)\big)/\big(N_\uparrow(E_F) + N_\downarrow(E_F)\big),$$

where $N_{\uparrow\downarrow}(E_F)$ is the spin-dependent density of states (DOS) at the Fermi level, E_F. Among various HM materials, fully compensated ferrimagnets (FCFM) are particularly attractive, e.g., for magnetic tunnel junction (MTJ) applications, as they do not produce stray magnetic fields. Several such materials have been reported in literature, including half-Heusler alloys such as CrMnSb, CrMnP, and CrMnAs, and others. In addition to the high degree of spin polarization, magnetocrystalline anisotropy (MCA) in magnetic thin films is another important parameter for applications in modern spin-based electronics, e.g., for magnetic data storage. In particular, MCA determines the orientation of magnetization direction, and thermal stability of magnetic materials. Perpendicular magnetic anisotropy (PMA) in thin films has attracted particular attention for various device applications, such as spin-transfer torque driven magnetization switching in magnetoresistive random-access memory (MRAM) [2, 3].

We perform density functional calculations, using the projector augmented-wave method (PAW), implemented in the Vienna *ab initio* simulation package (VASP) within the generalized-gradient approximation (GGA). The integration method with a 0.05 eV width of smearing is used. The cut-off energy of the plane-waves is set to 500 eV. Structural optimization is performed with the energy convergence criteria of 10^{-2} meV, which results in the Hellmann-Feynman forces being less than 0.005 eV/Å. The total energy and electronic structure calculations are performed with a stricter convergence criterion of 10^{-3} meV. The Brillouin zone integration is performed with a k-point mesh that results in a good convergence of the reported results. Some results and figures are obtained using the MedeA® software environment. Most of the calculations are performed using Extreme Science and Engineering Discovery Environment (XSEDE) resources located at the Pittsburgh Supercomputing Center (PSC), and the resources of the Center for Functional Nanomaterials (CFN) at Brookhaven National Laboratory (BNL). The magnetocrystalline anisotropy energy (MAE) is estimated as the difference of total energies calculated self-consistently for the magnetization pointing along the x and z directions ($MAE = E_x - E_z$) in the presence of spin-orbit coupling (SOC). Thus, a positive MAE indicates out-of-plane magnetization orientation, i.e., perpendicular magnetic

† s.poddar@euclidtechlabs.com

ISBN: 978-3-95450-214-1 ISSN: 2673-5490 doi:10.18429/JACoW-IPAC2021-WEPAB102

anisotropy, while a negative MAE indicates in-plane magnetization.

In the first approach a non-magnetic atom (Sb in CrMnSb), is replaced with another non-magnetic atom of smaller atomic radius. This should reduce the volume of the unit cell and could potentially shift the Fermi level inside the minority-spin energy band gap, thus inducing a half-metallic transition. We perform DFT for the most stable γ- phase (Fig. 1 (a)). Figure 1 (b) shows calculated total DOS as a function of "*x*" in $CrMnSb_{(1-x)}P_x$. At 50% P concentration, the half-metallic behavior is very robust, while further increase of the P content results in reduction of the minority-spin energy gap, with a transition to non-spin-polarized state at 100% P substitution. This is due to the quenching of the local magnetic moments under reduction of the unit cell volume [4].

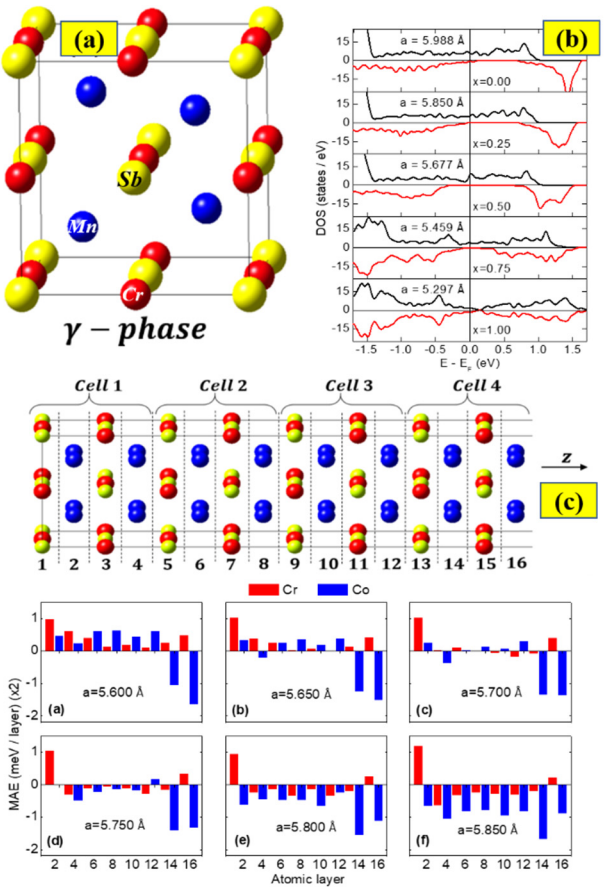

Figure 1: (a, b) γ-phase unit cell and DOS with P substitution, (c) layer resolved MAE.

In the second approach, we investigated the orientation of the spin moments in the spin filter layer. Fig. 1 (c) shows the 64-atom super cell of the Co_2CrAl, with layer resolved MAE in the bottom panel for different epitaxial strain [5]. The two main findings are as follows:

1. *Half-metallicity in certain Heusler alloys (CrMnSb) can be induced by chemical substitution*. In case of CrMnSb, chemical substitution induced half-metallicity is combined with fully compensated ferrimagnetism.
2. *In some Heusler compounds (Co_2CrAl) surface half-metallicity can co-exist with perpendicular magnetic anisotropy*. To the best of our knowledge, there are no earlier reports of half-metallic thin-film surfaces with PMA.

HM/GAAS DEVICE FABRICATION

Heusler alloy films (~5 nm) were grown in a VG V80 MBE system on nearly lattice-matched n-doped GaAs. 2 μm thick n-GaAs were grown on unintentionally doped (UID) GaAs buffer layers (200 nm) epitaxial grown on n-doped Si (001) substrates. The nGaAs/UID-GaAs stacks were grown in a separate conventional III-V MBE system and then arsenic capped and transferred through air into a dedicated metals MBE system for growth of the Heusler layers. We chose to grow Co_2FeSi and Co_2MnSi in our Phase I investigation primarily due to their close lattice matching with GaAs and highest magnetic moments as listed in Table 1.

Table 1: Co-based Heusler Alloys

Heusler Alloy	Curie T (K)	Magnetic Moment (μB)	Lattice Mismatch with GaAs (%)
Co_2FeSi	**1100**	**5.46**	**0.08**
Co_2FeAl	1000	4.98	1.3
Co_2MnSi	**985**	**5.0**	**0.3**
Co_2MnGe	905	5.0	1.6
Co_2MnAl	726	4.0	1.8

HARDWARE REQUIREMENTS

Originally a long stainless-steel stalk (radius = 1 inch) with brazed molybdenum disk at the end was used. The samples were bonded to stalk-end with indium and finally secured with an annular tantalum disk. The chamber had to be vented for each swap, unsuitable for sensitive samples, and baking cycles were long. To address these challenges, the mount was modified with copper beryllium (CuBe) Omicron-type drawer receptacle. A small vacuum suitcase was commercially obtained from Scienta-Omicron for sample transfers. It has 6-spring secured sample storage racks, a non-evaporable getter (NEG) plus ion combination pump, and a magnetically coupled wobble stick with bayonet style gripper with ±22° tilt, continuous 360° axial rotation and maximum throw of 485 mm (Fig. 2).

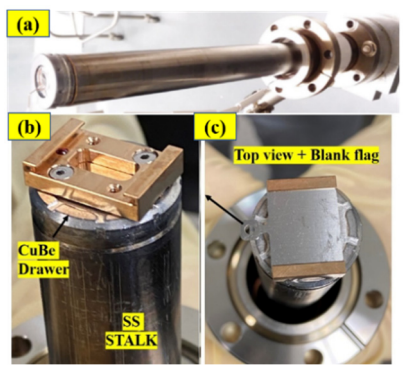

Figure 2: (a) Conventional and (b, c) modified mount.

ISBN: 978-3-95450-214-1 ISSN: 2673-5490 doi:10.18429/JACoW-IPAC2021-WEPAB102

MOTT POLARIMETRY RESULTS

Quantum efficiency, a ratio of the emitted electrons to incident photons, is measured by determining the photocurrent for a given incident laser power. Electron spin polarimeters like the Mott polarimeter take advantage of spin-dependent scattering processes to resolve spins and precisely measure the magnitude of an asymmetry also proportional to the net polarization. We used only the left/right (L/R) electron channel [6, 7]. Normal incidence of unpolarized light was used for all the preliminary data presented (Fig. 3).

The samples were transferred from the parking racks inside the vacuum suitcase to the modified stalk. They were biased with respect to the Mott polarimeter (-260 V to -270 V) and were activated with cesium (10 mins, 5 Amp runs, SAES Getters St-101 AMD). The photocurrent for as-grown Co_2FeSi/GaAs was measured first with no cesiation and then with cesiation (Fig. 4 (a)). The QE was repeated after letting the photocathode sit in the chamber overnight which yielded a measurable photocurrent. This is clear evidence of photoemission from the spin-filter device although the QE is an order of magnitude lower than the conventional GaAs photocathodes in the visible spectrum.

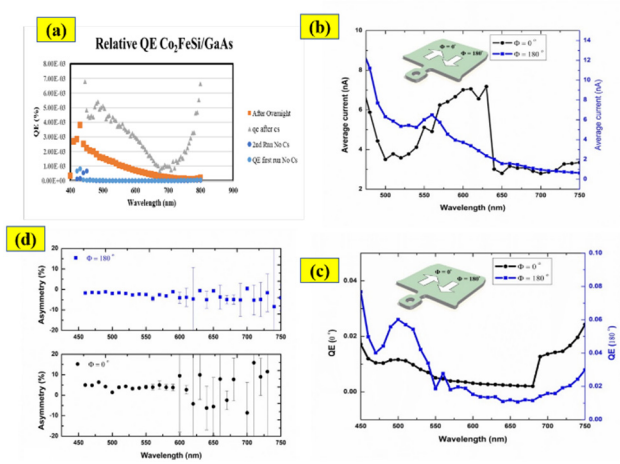

Figure 3: Average current and Quantum efficiency for as-grown (a) and magnetically switched spin-filter (b, c); (d) total asymmetry for two azimuthal directions of magnetic Co2FeSi/GaAs spin-filter.

The RHEED pattern suggests that the magnetization direction is in-plane along the tab direction of the sample flag holder. Accordingly, the magnetization direction was switched in the azimuthal plane ($\Phi = 180°$) and back ($\Phi = 0°$) using a low magnetic field. The QE signal improved compared to the as-grown sample indicating that the application of magnetic field assists in spin ordering of the half-metal layer. It is clear from Fig. 4 (b), that we have photoemission signature from both orientations of the spin-filter possibly due to spin-selective photoemission. The asymmetry from L/R channels is stable for $\lambda < 600$ nm but measurement uncertainty grows for higher wavelength which could be due to imperfect electrostatic lens steering or unaccounted background noise. The asymmetry also switches sign for the azimuthal direction, again a strong evidence of spin-filtering. The estimated polarization could be as high as 60-70% if we compare our level of asymmetry to standard photocathodes tested with similar system.

The second set of samples composed of 5 nm of epitaxial layer Co_2MnAl on GaAs was activated and a normal incidence of light was used for QE measurements (Fig. 4).

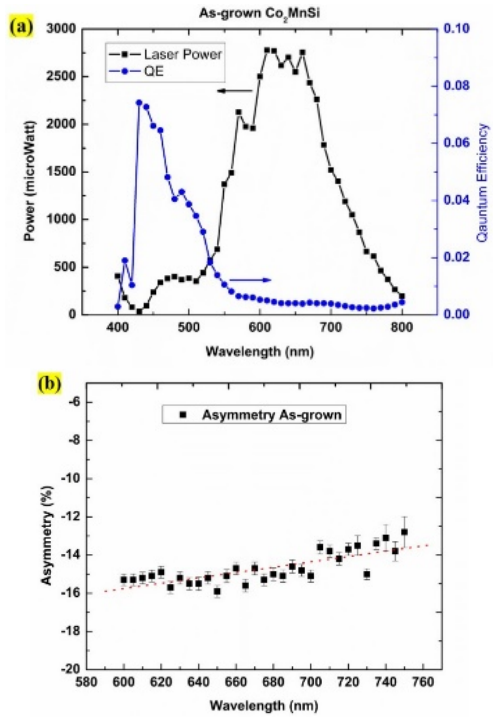

Figure 4: (a) QE spectral response and (b) asymmetry for as-grown Co2MnSi/GaAs spin-filter.

CONCLUSION AND FUTURE WORK

DFT studies predicted 100% magnetic spin polarization for elemental substitution and role of PMA on surface states. The HM surface states are chemically stable and does not alloy with Cs during activation. Upgraded sample holder design reduced the preparation time for polarimetry by 50%. QE 1-order of magnitude smaller than the conventional GaAs sources but enough to carry out polarimetry is achieved.

Spin polarized electrons are produced using linearly polarized light with magnetization direction of the spin-filter used as tuning parameter instead of the handedness of the circular polarized light. Qualitative difference is observed in the asymmetry data, but quantitative analysis of polarization needs major polarimetry hardware development which will be carried out in an ongoing work.

ACKNOWLEDGEMENTS

This work was supported by a Small Business Innovation Research grant to Euclid Beamlabs, LLC, from the U.S. Department of Energy, Office of Science, Office of Basic Energy Sciences, under grant number DE-SC0020564.

ISBN: 978-3-95450-214-1 ISSN: 2673-5490 doi:10.18429/JACoW-IPAC2021-WEPAB102

REFERENCES

[1] A. Hirohata *et al.*, "Heusler alloy/semiconductor hybrid structures", *Current Opinion in Solid State and Materials Science*, vol. 10, pp. 93-107, Apr. 2006. doi:10.1016/j.cossms.2006.11.006

[2] C. J. Palmstrøm, "Epitaxial Heusler Alloys: New Materials for Semiconductor Spintronics", *MRS Bulletin*, vol. 28, pp. 725-728, Oct. 2003. doi:10.1557/mrs2003.213

[3] C. J. Palmstrøm, "Heusler compounds and spintronics", *Progress in Crystal Growth and Characterization of Materials*, vol. 62, pp. 371-397, Jun. 2016. doi:10.1016/j.pcrysgrow.2016.04.020

[4] E. O'Leary *et al.*, "Chemical substitution induced half-metallicity in CrMnSb(1−x)Px", *Journal of Applied Physics*, vol. 128, p. 113906, Sep. 2020. doi:10.1063/5.0021467

[5] R. Carlile *et al.*, "Perpendicular magnetic anisotropy in half-metallic thin-film Co2CrAl", *Journal of Physics: Condensed Matter,* vol. 33, p. 105901, Mar. 2020. doi:10.1088/1361-648x/abd052

[6] K. Aulenbacher *et al.*, "Precision electron beam polarimetry for next generation nuclear physics experiments", *International Journal of Modern Physics E,* vol. 27, p. 1830004, Jul. 2018. doi:10.1142/s0218301318300047

[7] J. M Grames *et al.*, "High precision 5 MeV Mott polarimeter", *Physical Review C*, vol. 102, p. 015501, Jul. 2020. doi:10.1103/physrevc.102.015501